electronics

MDPI

Article

A New Method of the Pattern Storage and Recognition in Oscillatory Neural Networks Based on Resistive Switches

Andrei Velichko *, Maksim Belyaev, Vadim Putrolaynen and Petr Boriskov

Institute of Physics and Technology, Petrozavodsk State University, 31 Lenina str., Petrozavodsk 185910, Russia; biomax89@yandex.ru (M.B.); vputr@petrsu.ru (V.P.); boriskov@psu.karelia.ru (P.B.)

* Correspondence: velichko@petrsu.ru; Tel.: +7-8142-63-5773

Received: 10 September 2018; Accepted: 18 October 2018; Published: 22 October 2018

Abstract: Development of neuromorphic systems based on new nanoelectronics materials and devices is of immediate interest for solving the problems of cognitive technology and cybernetics. Computational modeling of two- and three-oscillator schemes with thermally coupled VO_2-switches is used to demonstrate a novel method of pattern storage and recognition in an impulse oscillator neural network (ONN), based on the high-order synchronization effect. The method allows storage of many patterns, and their number depends on the number of synchronous states N_s. The modeling demonstrates attainment of N_s of several orders both for a three-oscillator scheme N_s ~650 and for a two-oscillator scheme N_s ~260. A number of regularities are obtained, in particular, an optimal strength of oscillator coupling is revealed when N_s has a maximum. Algorithms of vector storage, network training, and test vector recognition are suggested, where the parameter of synchronization effectiveness is used as a degree of match. It is shown that, to reduce the ambiguity of recognition, the number coordinated in each vector should be at least one unit less than the number of oscillators. The demonstrated results are of a general character, and they may be applied in ONNs with various mechanisms and oscillator coupling topology.

Keywords: oscillatory neural networks; pattern recognition; higher order synchronization; thermal coupling; vanadium dioxide

1. Introduction

Usage of artificial neural networks [1] for information processing allows mastering the problems that arise when traditional computation schemes are applied in such areas as pattern and speech recognition [2], and data computation and encoding [3]. Therefore, the important research trends include studying the modes of oscillator neural network (ONN) operation and training, implementation of associative memory modes based, for example, on weakly coupled phase oscillators (Kuramoto model) [4] or impulse oscillators [5,6]. The effect of synchronization plays a crucial role in ONN operation, and is often used as a marker of ONN action, for example, in pattern recognition event.

There is a class of ONNs based on relaxation oscillators that generate subsequent pulses (spikes). These oscillators, in turn, are composed of electronic components with resistive switching effect, for example, VO_2-switches [7,8], 1T-TaS_2 charge density wave devices [9–11], thyristors [12], tunneling diodes [13], resistive memory elements [14], spin-torque nano-oscillators [15]. Such ONNs appear to be interesting because of hardware solution simplicity, as well as compactness and energy efficiency of the developed micro- and nanoelectronic self-oscillators. VO_2-based oscillators, as the elements of ONNs, have been chosen because they ensure rapid electric switching (~10 ns) [16], manufacturability with high degree of nanoscaling [17] and, above all, because of the pronounced effect of thermal

coupling that simplifies ONN assembly and circuit engineering of galvanically isolated oscillators. Consequently, VO_2-oscillators started being used as the prototypes of neuro-oscillators for cognitive technology [8,16,18].

In ONNs, the system demonstrates frequency and phase synchronization [19–22] and, also, synchronization of high order [17,23] at certain control parameters, such as parameters of an oscillator scheme or coupling strengths between the oscillators. The method proposed, here, of pattern storage and recognition, is based on the effect of high-order synchronization, that has been experimentally demonstrated through thermally coupled VO_2-oscillators [17]. In many studies [22,24,25], patterns to be stored are expressed through a set of vectors. Vector coordinates contain information about the pattern and unambiguously associate it with one of possible variants. For instance, the vector of the object's color in RGB coordinates (white color—RGB (255,255,255)) may be used as a 3-dimension vector. There are some methods of vector storage based on oscillator elements' synchronization in ONNs, and one of them is presented in paper [20]. To store **E** vector, a phase-shift keying method of a test vector **T** is specified by weight matrix setting; at the second stage, the weights are sharply changed to the initial values (corresponding to the stored vectors), and the system arrives at one of the stable combinations of phase shift **E**. However, this phase method has the following drawbacks: N^2 couplings with tunable weights and a two-stage procedure of pattern recognition.

A second known method of vector storage is a frequency-shift keying method of encoding, based on synchronized frequency shift [22]. According to this method, vector **E** is stored through oscillator frequency shifts against the central frequency of oscillator array F^0 synchronization (on the first harmonic) per the values corresponding to the vector coordinates $\mathbf{E} = (\delta_{\omega 1}, \delta_{\omega 2}, \ldots, \delta_{\omega \mathrm{N}})$. Recognition of test vector **T** occurs at the reverse shift of frequencies and, in the case when the vectors coincide $\mathbf{T} \approx \mathbf{E}$, the synchronization, indicating the fact of pattern recognition, takes place. This method allows usage of an oscillator star configuration and only N couplings, however, the disadvantage of this method is that just one vector is stored.

The present work suggests a conceptually new method of vector (pattern) storage and recognition when an array of coupled oscillators enables storage of a multitude of vectors. This result is achieved due to the effect of high-order synchronization in our ONN, that has many oscillator synchronous states and, also, because of specific algorithm of the network training and identification of the degree of match for the tested objects.

2. Materials and Methods

2.1. General Principle

An oscillator neural network is a system of N coupled oscillators, which may be connected via electric (by resistors and capacitors) [7,26], thermal [17], and optic [27] couplings, depending on the physical mechanism of oscillator interaction. In the general case, there is a matrix of coupling strengths $\Delta_{i,j}$ (weights), where i, j are the numbers of interacting oscillators, and $\Delta_{i,j}$ denotes the value of the i-th oscillator effect on the j-th one. Oscillator networks may form various topologies: fully connected—all-to-all; and not fully connected—bus, star, and ring. Figure 1a–c show examples of two and three oscillators connections using topologies "star", "all-to-all", and an example of N oscillator connections using a mixed topology (Figure 1d).

It is known [17,23] that oscillators in a network may undergo the effect of synchronization and, besides synchronization on the first harmonic, synchronous modes of high order may be observed if the signal spectra possess several harmonics. To evaluate synchronization, in this work, we use a family of metrics that consists of two parameters (SHR is the value of high order synchronization and η is the effectiveness of synchronization). A detailed method of its determination is given in Section 2.3 and in [17].

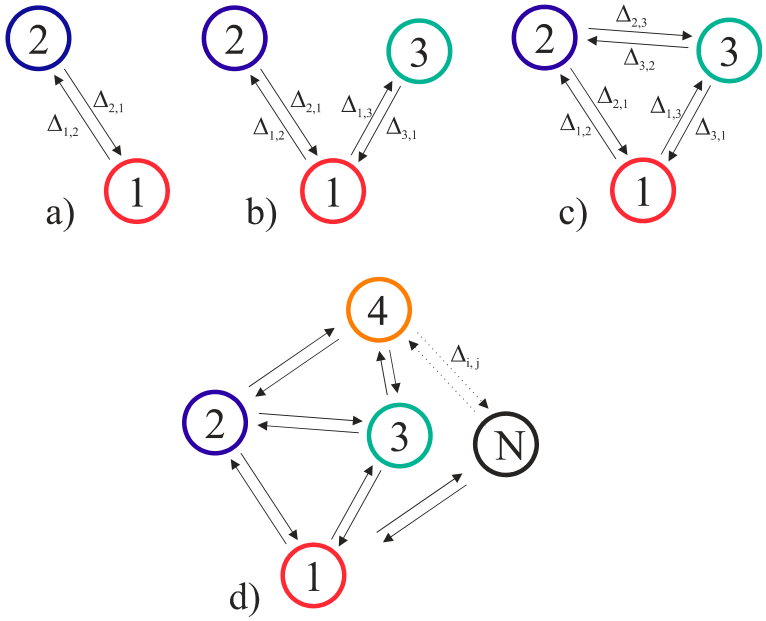

Figure 1. Examples of two (**a**) and three (**b**) oscillators connection into a neural network using topologies "star" (**b**), "all-to-all" (**c**), and *N*-oscillators using mixed topology (**d**), where $\Delta_{i,j}$ indicates the value of the *i*-th oscillator effect on the *j*-th one.

In the general case, high-order synchronization is determined by the ratio SHR = k_1:k_2:k_3:...:k_N, where k_N is a harmonic order of *N*-th oscillator at the common frequency of the network synchronization F_s, (SHR—subharmonic ratio). As an example, Figure 2 shows spectra of three electric oscillators that have synchronization of the order SHR = k_1:k_2:k_3 = 3:6:4. The following rule should be noted: if all paired oscillators have different synchronization frequencies, there is always a common synchronization frequency F_s for the whole system (all pairs), and the network synchronous state will also be determined by the ratio SHR = k_1:k_2:k_3:...:k_N at frequency F_s (see Section 2.3).

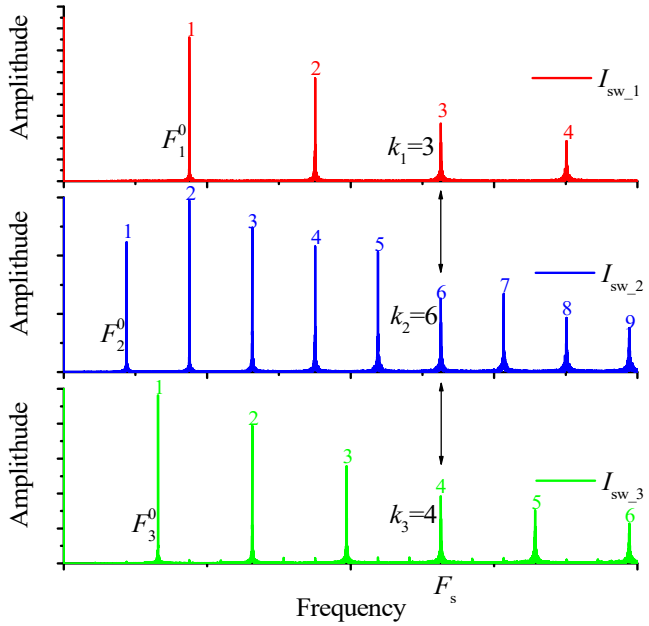

Figure 2. Example of oscillation spectra of three electric oscillators at synchronization order subharmonic ratio (SHR) = k_1:k_2:k_3 = 3:6:4, where I_{SW} is the current amplitude of a signal in an oscillator, F^0 is first harmonic, *k* is the harmonic number at the synchronization frequency F_s.

In addition to SHR, there is also a parameter of synchronization effectiveness η, that shows what share of oscillations of the whole time signal is synchronized. This parameter is expressed in percentages (see Section 2.3). If, at any point, η is less than the threshold value η_{th}, then SHR is absent, and the signal is considered conventionally non-synchronized.

Transition from one synchronous state into another is possible when the oscillator network control parameters are varied. For example, in electric oscillators, the main parameters may be oscillator feed currents I_{p}, their variation causes changes of the basic oscillation frequency F^0. Nevertheless, in some cases, transition between states may be achieved by variation of coupling forces or noise intensity.

The range of control parameters variation, where synchronization does not change its state, is called a synchronization area. There is a whole family of synchronization areas that are called Arnold's tongues (for the case of two oscillators). A schematic example of synchronization areas for a three-oscillator scheme is shown in Figure 3a. Here, the control parameters are oscillator feed currents. Each area has its own value of SHR. Besides, each area has its own distribution of the synchronization effectiveness value within $\eta_{\text{th}} < \eta < 100\%$, with a peaked curve.

The number of possible variants of synchronous states (synchronization areas), where the system may exist when the basic control parameters are varied, is denoted as N_{s}. The value of N_{s} depends on many parameters: the oscillator number N, the range of control parameters and their number, network topology, strength of coupling between oscillators, noise level in the system and on the threshold value of synchronization effectiveness η_{th}. We will cover the issue in detail later, nevertheless, we have shown in [28], that for a two-oscillator network, N_{s} has a maximum at certain values of coupling strengths between oscillators, and decreases when the system noise amplitude increases. When the coupling strength grows considerably, the value N_{s} decreases because of the nearby synchronization areas' integration.

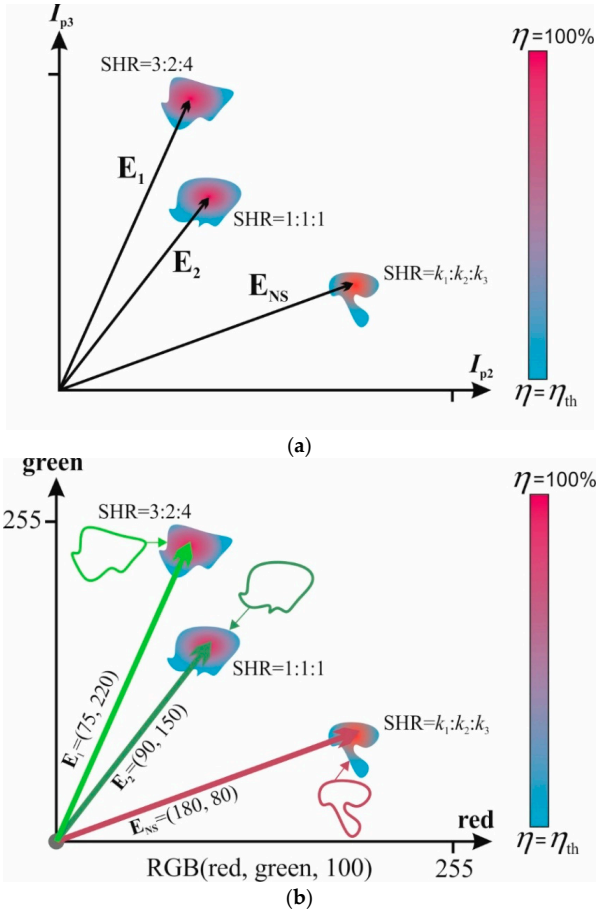

Figure 3. *Cont.*

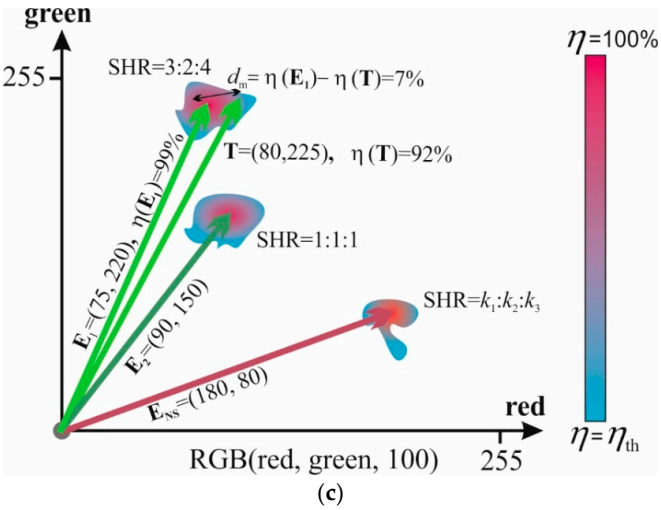

Figure 3. (**a**) Schematic representation of the synchronization areas for a three-oscillator scheme; (**b**) Examples of the vector and object's RGB color association, that illustrate the algorithm of the network training and recognition (**c**).

Vectors $\mathbf{E}_1$, $\mathbf{E}_2$, ..., $\mathbf{E}_{NS}$, that connect the origin of coordinates with the points of synchronization effectiveness maximum η, can be associated with the synchronization areas. Thus, the system stores N_s of vectors, and the dimensionality of the stored vectors M is determined by the number of chosen control parameters. The coordinates determine the shift of oscillators' control parameters, for example, currents $\mathbf{E} = (\delta I_{p1}(1), \delta I_{p2}(2), \ldots, \delta I_{pN}(M))$, against the origin of coordinates.

As we have mentioned in the introduction section, the patterns to be stored are usually expressed through a set of vectors. Vector coordinates contain information about the pattern and unambiguously associate it with one of possible variants. For example, Figure 3c shows storage of the object's colors in the RGB format (red, green, blue) through the coordinates of vectors **E,** whose values give the information about the intensity of red and green colors **E** = (red, green), and parameter blue is fixed as blue = 100. This example, in Figure 3c, shows the intensities of RGB components on the axes that can be linearly transformed into the values of the oscillator currents and vice versa.

We suggest the following methods of pattern storage and recognition in a neural network, based on the high-order synchronization effect, and its general scheme is given in Figure 4.

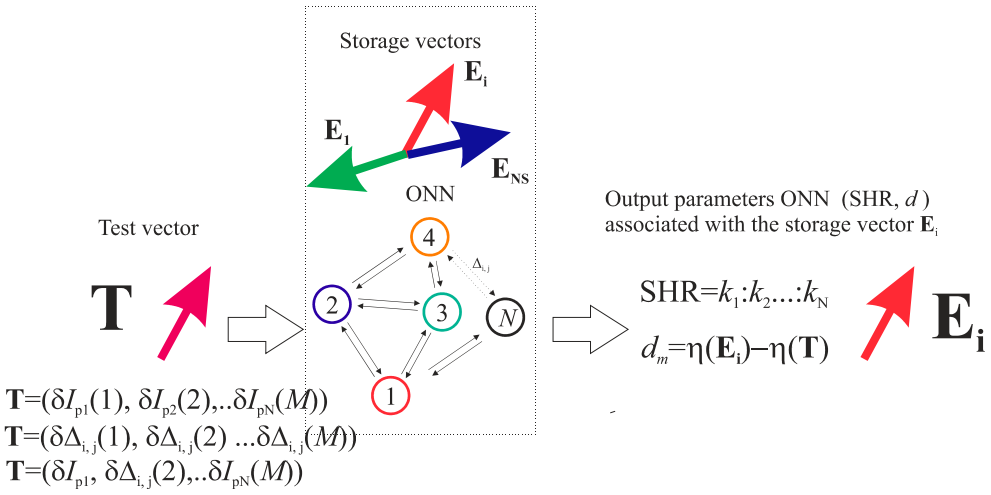

Figure 4. Schematic representation of pattern recognition principle by using oscillator neural network (ONN), where M is the dimensionality of the test vector **T**, N is the number of oscillators, N_s is the maximal number of the stored vectors **E**.

2.1.1. Vector Storage and ONN Training

The general algorithm for vector storage and ONN training includes the following steps:

1. For storage, arbitrary vectors $\mathbf{E}_1$, $\mathbf{E}_2$, ... , $\mathbf{E}_i$, ..., $\mathbf{E}_{Ns}$ should be specified. If necessary, control parameters should be transformed into the corresponding coordinate system (for example, a color one, see Figure 3b,c). In general, vectors have dimensionality M and appear as a set of a network parameters that affects the system SHR. For example, they can be either currents, as shown in Figure 3 $\mathbf{E} = (\delta I_{p1}(1), \delta I_{p2}(2), \ldots , \delta I_{pN}(M))$, or they can be coupling strengths between some definite oscillators $\mathbf{E} = (\delta\Delta_{i,j}(1), \delta\Delta_{i,j}(2), \ldots , \delta\Delta_{i,j}(M))$, or mixed parameters $\mathbf{E} = (\delta I_{p1}(1), \delta\Delta_{i,j}(2), \ldots , \delta\Delta_{i,j}(M))$ (see Figure 4).
2. Then, the network should be trained by the adjustment of the ONN parameters that are not used for the vectors' determination (coupling strengths, currents of other oscillators in the network, noise level, and synchronization effectiveness threshold η_{th}). The adjustment is performed until the synchronization areas coincide with the vectors' ends at the point of maximum value of synchronization effectiveness η (similar network training was used in the work [15]). The adjustment can be performed in two steps.
    a. First, by using random search until the vectors enter the synchronization area.
    b. Then, one of gradient methods [29] may be applied to search the maximum η. As a result, each stored vector corresponds to its unique value of SHR and maximum of $\eta(\mathbf{E})$.
3. If the training does not provide a positive result, one more oscillator should be included into the system and coupled with all oscillators already present, thus increasing the number of varied parameters and the number of possible synchronous states N_s. Then, the training should be repeated (see step 2).

2.1.2. Vectors Recognition

The algorithm of test vector $\mathbf{T}$ recognition includes the following steps:

1. Set the test vector $\mathbf{T}$ to the system input through applying shifts to the control parameters (see Figure 4). The vector's coordinates may be either shifts of currents, or coupling strengths or their combination, as it has been indicated above.
2. If one of the conditions is met ($\mathbf{T} \approx \mathbf{E}_1$ or $\mathbf{T} \approx \mathbf{E}_2$ or ... or $\mathbf{T} \approx \mathbf{E}_{NS}$), i.e., coordinates values of $\mathbf{T}$ are equal to one of the stored patterns, a transition to the synchronous state will occur and, actually, the act of the corresponding pattern recognition will take place. Which patterns have been exactly recognized can be determined by the value of SHR. The existence of the synchronization areas ensures the vector recognition even at its coordinates' insignificant displacement from the stored pattern.
3. The degree of match d_m between the objects may be such magnitude as the difference between the synchronization effectiveness of the stored and the test vectors $d_m = \eta(\mathbf{E}) - \eta(\mathbf{T})$. If the magnitude of $\eta(\mathbf{E})$ is not known, then to compare the degree of match, the formula $d_m = 100\% - \eta(\mathbf{T})$ can be used. The less d_m is, the closer vector $\mathbf{T}$ is to vector $\mathbf{E}$.

This method is a more complicated version of the method described in [22], where the analogy to the frequency-shift keying method of coding is used and, instead of setting the vector through frequencies $\mathbf{E} = (\delta\omega_1, \delta\omega_2, \ldots , \delta\omega_N)$, in our method, the vector is set through the control parameters $\mathbf{E}_1 = (\delta I_{p1}, \delta I_{p2}, \ldots , \delta I_{pN})$, that has the same meaning. The principle difference is that here, a high-order synchronization effect is used, thus allowing storage of a multitude of patterns in the ONN.

Besides, as described in the results section, it is more practical to use vector dimensions $\mathbf{E'} = (\delta I_1, \delta I_2, \ldots , \delta I_{N-1})$ with one less than the number of oscillators $(N - 1)$.

2.2. Model Object

As a model object, we have chosen a neural network composed of three thermally coupled VO_2-oscillators, where each oscillator has the scheme of a relaxation oscillator. Our choice is conditioned by the fact that we have done some research in thermal coupling [17,30] and its modeling, however, the coupling may be an electric one (capacitive or resistive [7]). It is known that an electric switching effect is observed in VO_2 film-based structures, that is conditioned by a phase metal–insulator transition (MIT) at the moment when the temperature reaches T_t ~340 K, because of Joule heating by the passing current I_{sw} [16]. This gives high-impedance (OFF) and low-impedance (ON) branches on I–V characteristics with threshold voltages ($OFF \rightarrow ON$) U_{th} ~5 V and holding voltages ($ON \rightarrow OFF$) U_h ~1.5 V (see Figure 5a). Both branches of I–V characteristics are reasonably well approximated by f_{sw} curve, consisting of two linearized regions with dynamic resistance R_{off} ~9.1 kΩ and R_{on} ~615 Ω:

$$I_{sw} = f_{sw}(U) \approx \begin{cases} \frac{U}{R_{off}}, State = OFF \\ \frac{(U - U_{bv})}{R_{on}}, State = ON \end{cases}, \quad (1)$$

where U_{bv} ~0.82 V is bias voltage of a low-impedance region, and *State* is a switch state.

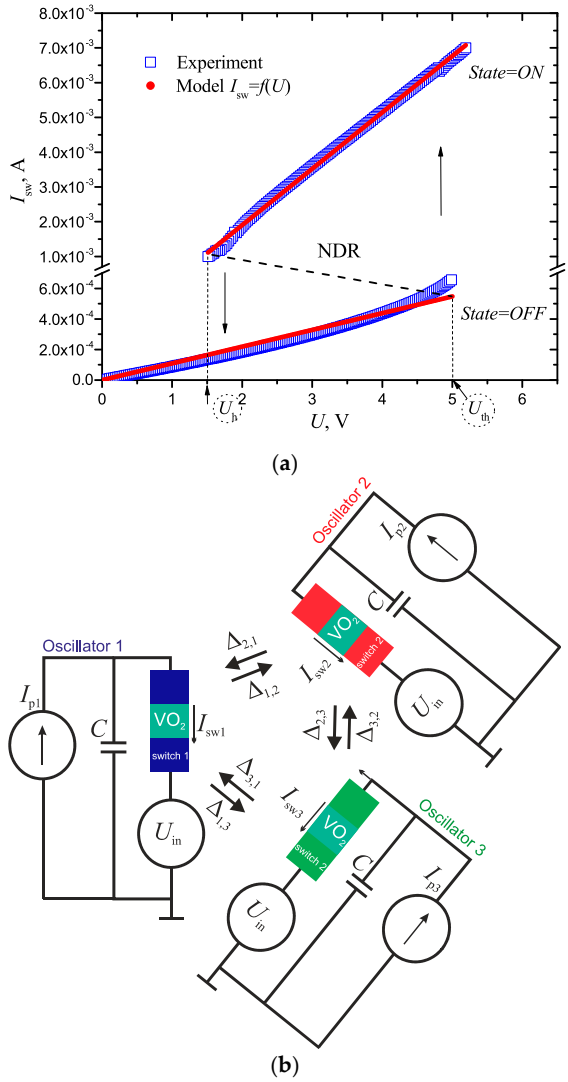

Figure 5. Experimental and model I–V characteristics of VO_2-switch (**a**); a model scheme of a neural network based on three oscillators circuits with VO_2-switches interacting via thermal coupling (**b**).

One of three topologies presented in Figure 1 may be realized, depending on coupling strength magnitudes Δ. At non-zero $\Delta \neq 0$, the topology is "all-to-all" (Figure 1c); at $\Delta_{2,3} = \Delta_{3,2} = 0$, the topology is "star" (Figure 1b); and at $\Delta_{2,3} = \Delta_{3,2} = \Delta_{1,3} = \Delta_{3,1} = 0$, the scheme turns into a two-oscillator one (Figure 1a). The control parameters here are source currents I_{p1}, I_{p2}, I_{p3}, and their variation leads to alteration of the fundamental oscillation frequency F^0 of oscillators.

Variations of each oscillator are described by the equation of Kirchhoff's law:

$$C\frac{dU_i(t)}{dt} = I_{p(i)} - I_{sw(i)}(t), \tag{2}$$

where $U_i(t)$ is the output voltage taken from the capacitor (C = 100 nF), $I_{sw(i)}(t) = f_{sw}(U_i(t) - U_{in})$ is the current passing through a switch, determined by I–V characteristics (1), $I_{p(i)}$ is the i-th oscillator supply current, respectively, U_{in} is the amplitude of switch internal noise, and i is the oscillator's number.

Thermal interaction between the i-th VO_2-oscillator and the neighbor ones ((i+)—clockwise and (i−)—counterclockwise of the scheme in Figure 5b) is realized according to the rule

$$U_{th(i)} = \begin{cases} U_{th(i)} - \Delta_{(i+),i}, \text{ if } State_{(i+)} = ON \\ U_{th(i)} - \Delta_{(i-),i}, \text{ if } State_{(i-)} = ON \\ U_{th(i)} - \Delta_{(i-),i} - \Delta_{(i+),i}, \text{ if } State_{(i-)} = State_{(i+)} = ON \end{cases}. \tag{3}$$

If the states of oscillators $State_{(i+)}$ and $State_{(i-)}$ are on the OFF branch of I–V characteristics, then the threshold voltage of the i-th VO_2-oscillator does not change: $U_{th(i)} = U_{th}$. Rule (3) is the same for all oscillators (with regard to cyclic permutation).

Oscillograms of oscillations with ~250,000 points and time interval δt = 10 μs were simulated using Equations (1)–(3). After that, the oscillograms were automatically processed, the synchronization order was determined, and cross-sections of oscillator synchronization areas were built.

The switch parameters did not change in numerical simulation of the results, but current intensities I_p, coupling strength Δ, and noise amplitude U_{in} varied.

2.3. Method of Calculating a Family of Metrics

To define the synchronization order, we used the family of metrics described above, that consists of two parameters SHR and η.

The problem of finding the high-order synchronization value determined by the ratio of integers SHR = k_1:k_2:k_3:...:k_N (see Section 2.1) may be solved in several ways. For example, by direct analysis of all oscillation spectra, or by searching the synchronization order of each pair of oscillators based on the method which we suggested in [17].

It should be noted that, at synchronous state, the frequency sets of fundamental (first) harmonics of oscillators ($F_1{}^0$, $F_2{}^0$, $F_3{}^0$, ... , $F_N{}^0$) must be commensurable. This is evident because at the synchronous state, there is a common synchronization frequency F_s, and the equality ($F_s = F_1{}^0 \cdot k_1 = F_2{}^0 \cdot k_2 = \ldots = F_N{}^0 \cdot k_N$) is fulfilled. If we divide $F_1{}^0$ into all frequencies in the set ($F_1{}^0$, $F_2{}^0$, $F_3{}^0$, ... , $F_N{}^0$), then we will get (1, $F_1{}^0/F_2{}^0$, $F_1{}^0/F_3{}^0$, ... , $F_1{}^0/F_N{}^0$) = (1, k_2/k_1, k_3/k_1, ... , k_N/k_1), that is, a new set of rational numbers determining pair synchronization of all oscillators in regard to the first oscillator (see [17]).

Thus, the method of specifying all values of k and the synchronization order of the system consisting of N-oscillators comes down to determining the set of pair synchronization fractional values (in regard to the first oscillator) for N-pairs (m_1/d_1, m_2/d_2, ... , m_{N-1}/d_{N-1}), and to its reduction to a common denominator:

$$\left(\frac{m_1}{d_1}, \frac{m_2}{d_2}, \frac{m_3}{d_3} \ldots \frac{m_{N-1}}{d_{N-1}}\right) \rightarrow \left(\frac{k_2}{k_1}, \frac{k_3}{k_1}, \frac{k_4}{k_1} \ldots \frac{k_N}{k_1}\right). \tag{4}$$

For example, a set of pair synchronization for oscillator pairs (№1–№2) and (№1–№3) in Figure 2 looks like (2/1, 4/3), after reduction to a common denominator (4), we get (2/1, 4/3) → (6/3, 4/3), and SHR = k_1:k_2:k_3 = 3:6:4.

It should also be noted that the algorithm of pair synchronization definition is based on the search of current oscillation peaks, I_{sw}, synchronous in time [17].

The effectiveness of pair synchronization η is determined as the percentage of the durability of all N_{SHR} synchronous periods T_s with the definite SHR, to the whole durability of the processed oscillogram T_{all}:

$$\eta = \frac{N_{SHR} \cdot Ts}{T_{all}} \cdot 100\% \quad (5)$$

If there are several synchronization types with different SHR, then the resulting η is associated with the maximum which, in turn, is compared with the threshold value η_{th} (in our case 90%). Oscillations are considered synchronized when η exceeds the threshold $\eta \geq \eta_{th}$. If the system consists of more than two oscillators, then the total effectiveness η is calculated as the mean value of all oscillator pairs. It should be noted that the proposed methods of SHR and η identification may be used in oscillator systems with noise. It has been noted that the noise increase leads mainly to the decrease of η, while SHR does not normally change.

3. Results

The results of synchronization areas modeling for a two-oscillator scheme (see Figure 1a) are given in Figure 6a. Control parameters are oscillator feed currents I_{p1}, I_{p2}, and noise and coupling strength values are U_{in} = 40 mV and Δ = 0.2 V. It can be seen that there is a whole family of synchronization areas that are called Arnold tongues [23]. The number of possible variants of synchronous states, N_s, in which the system may exist while the control parameters are varied, is N_s = 9. The dimension of the stored vectors in this case is 2, and the coordinates determine current shifts $\mathbf{E}_1 = (\delta I_{p1}, \delta I_{p2})$, with respect to the origin of coordinates.

The problem here is that the synchronization areas are long-ranged (of Arnold's tongues shape) therefore, there is a wide range of stored pattern coordinates which bring the system into a certain synchronous state. The solution lies in narrowing the dispersion of stored pattern coordinates by using vectors $\mathbf{E'}_1 = (\delta I_1, \delta I_2, \ldots, \delta I_{N-1})$ of a dimension one less than the number of oscillators $(N - 1)$, in this case, $\mathbf{E'}_1 = (\delta I_1)$. In practice, this means that we fix the current for one oscillator, and vary the currents for the others (see Figure 6a, dashed line I_{p2} = const). Thus, we eliminate the ambiguity of synchronization definition by one of the vector coordinates, and the areas of possible synchronization are narrowed.

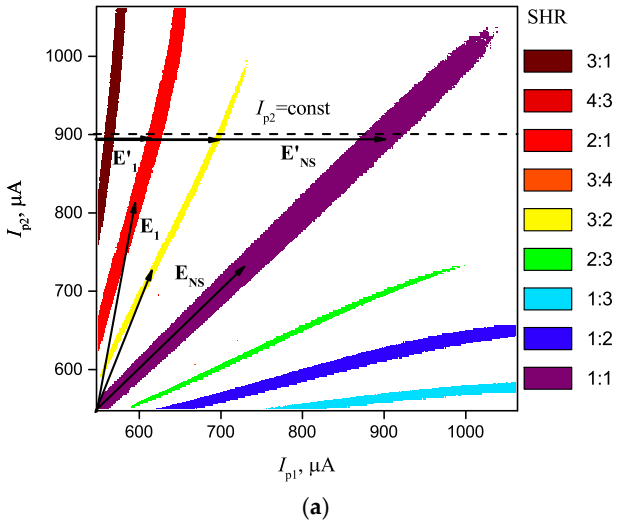

(**a**)

Figure 6. *Cont.*

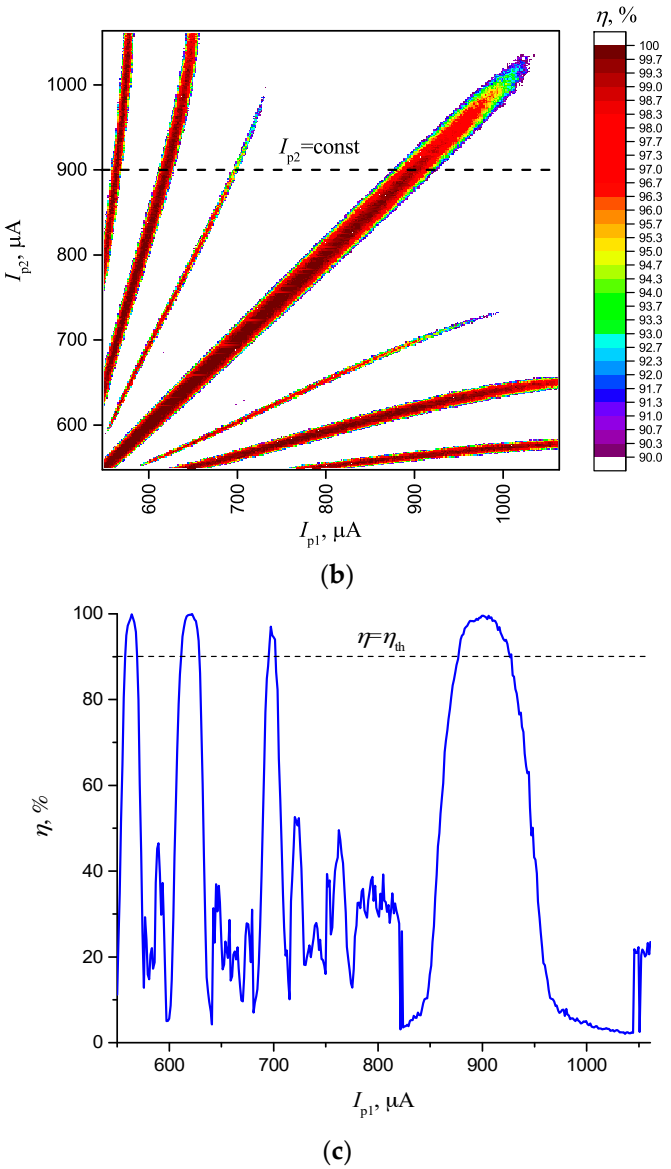

Figure 6. Example of synchronization areas for a two-oscillator scheme (**a**). The arrows show sampled vectors **E** and **E′**, in regard to the origin of coordinates. Distribution of η for a two-oscillator scheme (**b**). Cross-section η at I_2 = 900 μA (**c**).

Figure 6b shows the distribution of synchronization effectiveness inside the Arnold's tongues. It can be seen that η falls down to the edges of synchronization areas, whereas maximum of η has a progressive form in the area of control parameters, and is placed in the line in the center. When a cross-section is made (shown in Figure 6c), we can observe local maximums of η inside the synchronization areas and this is another argument to use the gradient search method in the algorithm of the network training. According to the above proposed method of recognition, the magnitude $d_m = \eta(\mathbf{E'}) - \eta(\mathbf{T})$ may serve as the parameter of the degree of match between the test and stored vectors.

Figure 7 shows cross-sections of synchronization areas for a system consisting of three oscillators ("star", see Figure 1b) at fixed current on the first oscillator I_{p1} = 950 μA, and parameters U_{in} = 40 mV and Δ = 0.2 V, that are similar to a two-oscillator scheme.

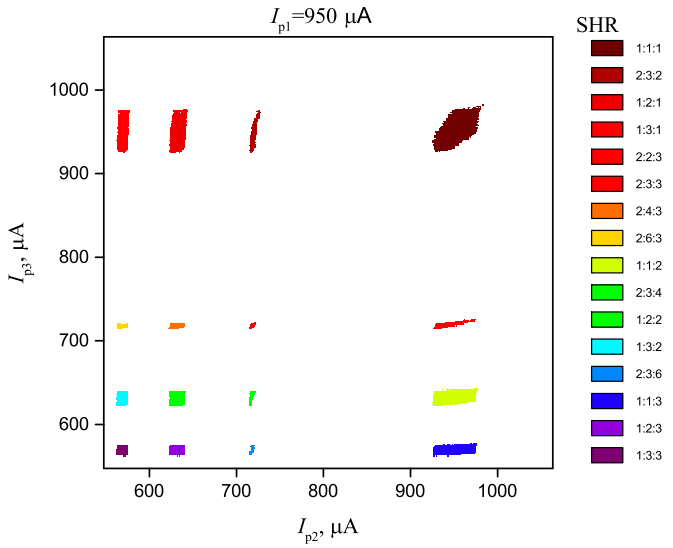

(**a**)

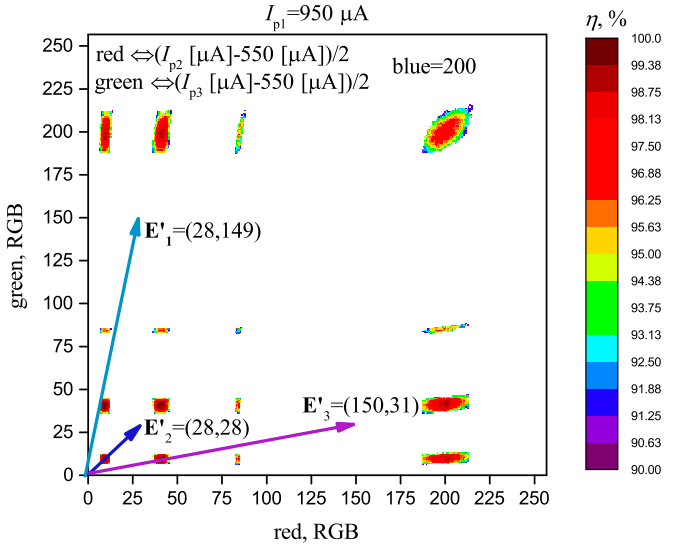

(**b**)

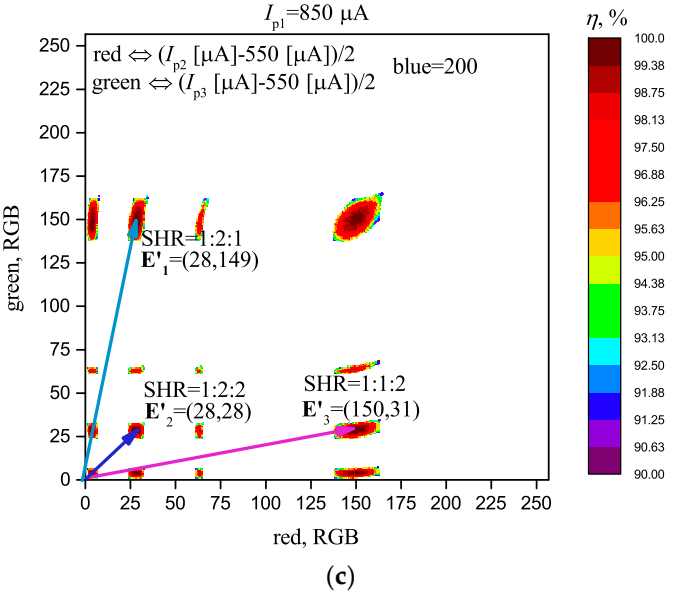

(**c**)

Figure 7. *Cont.*

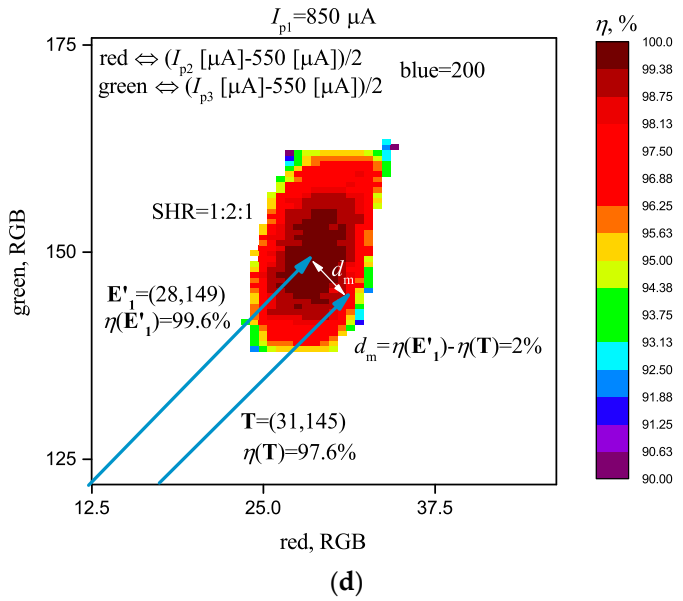

Figure 7. (**a**) Synchronization areas with SHR for a three-oscillator scheme "star" at I_{p1} = 950 μA; (**b**) Distribution of synchronization effectiveness η with the set vectors **E′** at I_{p1} = 950 μA; (**c**) Distribution of synchronization effectiveness η with the set vectors **E′** at I_{p1} = 850 μA, on an enlarged scale with vector **T** (**d**); Levels of coupling Δ = 0.2 V and noise U_{in} = 40 mV.

It can be seen that the synchronization areas are separate isolated regions that are suitable for setting vectors **E′** of dimension 2. In this case, with all other things being equal, N_s depends on the topology, and is N_s = 16 for a "star" connection and N_s = 14 for an "all-to-all" connection. The area shape also depends on the topology.

When comparing the values for two- and three-oscillator schemes with the same parameters, including the topology, we may propose a general rule stating that with the increase of the number of interacting oscillators, N_s, increases. Yet, this is evident as the number of freedom degree increases at determining the synchronization value SHR = k_1:k_2:k_3:...:k_N. Nevertheless, as we show below, at certain parameters, there are some exceptions from the general rule.

Distribution of synchronization effectiveness is shown in Figure 7b. Here, we can see that a local maximum η is present in each area, and it can be used for vector storage and recognition, according to the method described in Section 2.1.

Below, we will give an example of a vector storage and recognition (that determine colors RGB) by using the algorithm described in Section 2.1 for the scheme "star".

3.1. Vector Storage and ONN Training

Step 1: Suppose that we have to store three vectors that correspond to three colors RGB at the constant level of the component blue = 200, with coordinates **E′**$_1$ = (28, 149), **E′**$_2$ = (28, 28), and **E′**$_3$ = (150, 31). It should be noted that the number of coordinates in each vector is one unit less than the number of oscillators, and is equal two. As it has been explained above, this is necessary to narrow the area of possible synchronization and to reduce the recognition ambiguity. Liner transformation of coordinates, from the current parameters into color parameters, should be thought over initially. In our case, we used the following formulas: red ⇔ (I_{p2} [μA] − 550 [μA])/2 and green ⇔ (I_{p3} [μA] − 550 [μA])/2. After the working area has been transformed, we set three vectors, as shown in Figure 7b.

Step 2: Then, we start the system training by adjusting parameters of the ONN (I_{p1} and coupling strength $\Delta_{i,j}$) in such a way that the synchronization areas are obtained on the vectors at the point of maximum η. A fine adjustment for the maximum η can be done by using the gradient search. As a result, we have found that at $\Delta_{i,j}$ = Δ = 0.2 V, and I_{p1} = 850 μA, the system complies with the assigned task.

Step 3: As we have achieved a positive result after the network training, the vector recording may be considered completed at this step.

3.2. Vectors Recognition

When test vector $\mathbf{T} \approx \mathbf{E'}_1$ is supplied, the neural network is transformed into a synchronous state with the synchronization order 1:2:1. At $\mathbf{T} \approx \mathbf{E'}_2$, we get SHR = 1:2:2. At $\mathbf{T} \approx \mathbf{E'}_3$, we get SHR = 1:1:2. In each case, the degree of match $d_m = \eta(\mathbf{E'}) - \eta(\mathbf{T})$ is calculated, that determines the degree of match of vector **T** with the stored vectors. For example, at **T** = (31,145), the system transfers to SHR = 1:2:1 and the vector is recognized as the vector $\mathbf{E'}_1$ = (28,149), with the degree of match $d_m = \eta(\mathbf{E'_1}) - \eta(\mathbf{T}) = 2\%$ (see Figure 7d).

Step 1: Set the test vector **T** = (31,145).

Step 2: Determine that the system transfers to SHR = 1:2:1, and the vector is recognized as the vector $\mathbf{E'}_1$ = (28,149).

Step 3: Determine the degree of match $d_m = \eta(\mathbf{E'_1}) - \eta(\mathbf{T}) = 2\%$.

Thus, we have performed storage and recognition of three various patterns with RGB color, although the capacity of this system is considerably higher and enables storing up to 16 patterns simultaneously.

Figure 8 shows the dependence of the number of synchronous states N_s on Δ at three different configurations of a neural network at the constant noise level U_{in} = 20 mV. The existence of the main maximum N_s is evident at some optimal value Δ_{opt}, in this case, this value is roughly the same as Δ_{opt} ~0.1 V for all configurations, and does not depend on the oscillator number. The existence of the curve maximum $N_s(\Delta)$ reduplicates our results obtained in [28] for a two-oscillator scheme. Inalterability of Δ_{opt} for a different number of oscillators N, with all other parameters being equal, might be explained by the fact that, with the increase of the number of freedom degrees for synchronization order, SHR = k_1:k_2:k_3:..:k_N, the value of N_s has the tendency to grow.

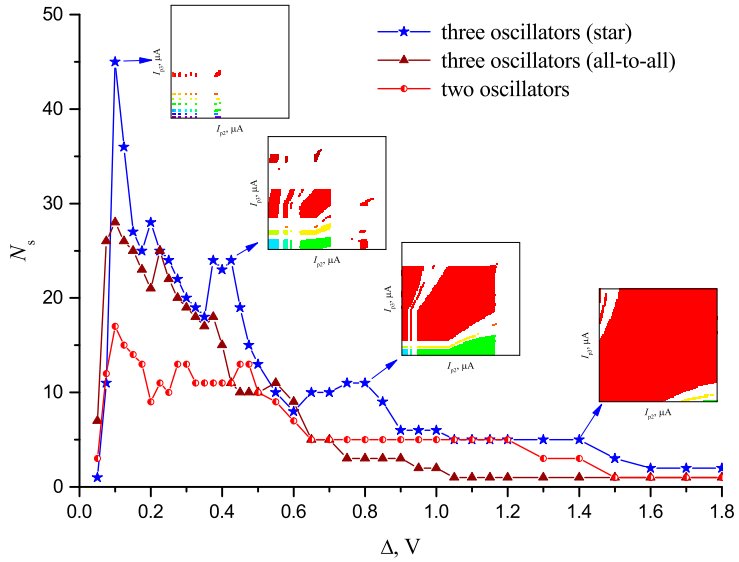

Figure 8. Dependence N_s on coupling strength value between oscillators Δ at various configurations of oscillator neural network and constant noise level U_{in} = 20 mV. The insertions show the evolution of synchronization areas and demonstrate the effect of their merging with Δ growth.

We should also note the general tendency for N_s to decrease when the coupling strength Δ grows above Δ_{opt} and, at its large values, the system tends to the lowest possible N_s = 1 with synchronization value 1:1:1. This is related to the fact that, with the increase of Δ, the surface of certain synchronization areas increase. Neighboring areas merge; in this case, the synchronization order of the resulting area

predominantly consists of lower harmonic numbers. As the dimension of the control parameters is limited, such growth of synchronization area surfaces irrevocably results in a decrease of their number and value of N_s. The insertions in Figure 8 show the evolution of synchronization areas and demonstrate the effect of their merging with Δ growth.

Besides, we should note the existence of local maximums at $\Delta > \Delta_{opt}$. In turn, this is related to the fact that, in the presence of noise in the neural network, the increase of Δ may result in the development of new synchronization areas at the control parameters values that previously corresponded to the non-synchronous state of the system. Therefore, in a general case, the curve $N_s(\Delta)$ may have a complicated shape with several maximums, as we can see in Figure 8.

In addition, the initial sharp growth of all three curves at the plot should be noted when Δ increases from 0 to Δ_{opt}. The latter is due to synchronization effect degradation at $\Delta \to 0$.

When comparing the curves, it may be noted that the increase of the oscillator number in the network leads to the increase of the maximum value of N_s in the system; this does not contradict the rule suggested above. For example, $N_{s\_max} = 17$ is for two oscillators, for three-oscillator schemes, and $N_{s\_max} = 28$ and $N_{s\_max} = 45$ are for the "all-to-all" and "star" schemes, respectively. At the same time, at certain values of coupling strength (for example, at $\Delta = 1.1$ V), the value of N_s for a two-oscillator scheme may be even higher. Also, the regularity that the "star" topology has higher N_s than the topology of "all-to-all" is observed. All of these things mean that the increase of the coupling number may contribute to the effect of system desynchronization and decrease of N_s, as it seems that oscillators prevent each other from synchronization.

Figure 9 shows the curve of N_s vs noise level in the system U_{in} at the same coupling strength $\Delta = 0.2$ V, for three configurations of an oscillator neural network. The general trend for the decrease of N_s at the noise amplitude increase is due to the decrease of the surface of synchronous areas which eventually disappear (see the insertions in Figure 9).

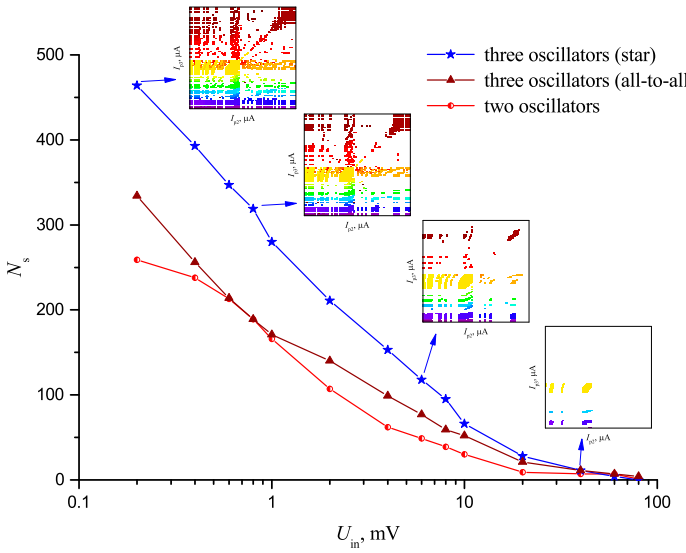

Figure 9. Dependence N_s on noise level U_{in} at various configurations of an oscillator neural network at the same coupling strength $\Delta = 0.2$ V.

It should also be noted that the general rule is observed: stating that the value of N_s for a three-oscillator configuration "star" is higher than that for a two-oscillator one. The shapes of curves $N_s(U_{in})$ are similar, which indicated that the physics of noise effect on the network is similar, and does not depend on the number of oscillators.

Comparing the above curves $N_s(\Delta)$ and $N_s(U_{in})$, it may be seen that the number of synchronization areas N_{s_max} in our models may reach N_{s_max} ~450, at an optimal coupling strength value $\Delta = \Delta_{opt}$, and at lowered noise $U_{in} = 10$ μV, it increases to $N_{s\_max} \sim 650$.

4. Conclusions

A new method of pattern storage and recognition in an impulse oscillator neural network based on resistive switches and the high-order synchronization effect is presented, using computational modeling of two- and three-oscillator schemes with thermally coupled VO_2-switches.

Our method allows storage of a multitude of patterns N_s, where each state of the system is characterized by synchronization order SHR = k_1:k_2:k_3:..:k_N.

A general rule is suggested, stating that N_s increases with the increase of the number of interacting oscillators. The modeling demonstrates achievement of N_s of several orders: N_s ~650 for a three-oscillator scheme and N_s ~260 for a two-oscillator scheme.

Several regularities of functional characteristics of such ONNs have been obtained; in particular, the existence of an optimal coupling strength between oscillators has been revealed, when the number of synchronous states is maximal. A general tendency for N_s decrease with the increase of coupling strength and switches' inner noise amplitude, is also shown.

The algorithm of vector storage, network training, and test vector recognition has been proposed, where the parameter of synchronization effectiveness is used as the degree of match. It has been shown that it is more expedient to use the number of coordinates in each vector at least one unit less than the number of oscillators ($N - 1$), because it is necessary to narrow the area of possible synchronization and to lower the recognition ambiguity.

By contrast, for example, to the FSK method [22], such an approach to the problem of pattern storage and recognition allows one to significantly increase the information capacity, N_s, of a neural network using the minimum number of neural oscillators. In addition, the proposed concept of pulse synchronization definition, through calculation of a family of metrics, opens a natural way for gradient method application to an oscillator network training (optimization).

Although the research has been performed on a certain model object (VO_2 thermally coupled relaxation oscillators), the demonstrated method of pattern storage and recognition is sufficiently general, and the fundamental character of the obtained regularities may be the subject of further research of ONNs, of various mechanisms and oscillator-coupling topology.

Author Contributions: Conceptualization, A.V. and M.B.; methodology, V.P. and P.B.; software, A.V.; validation, P.B.; writing—original draft preparation, A.V., M.B. and V.P.; project administration, A.V.

Funding: This research was supported by Russian Science Foundation (grant no. 16-19-00135).

Acknowledgments: The authors express their gratitude to O. Dobrynina for some valuable comments in the course of the article translation.

Conflicts of Interest: The authors declare no conflict of interest.

References

1. Heaton, J. *Artificial Intelligence for Humans*; Createspace Independent Publishing: Scotts Valley, CA, USA, 2015; ISBN 9781505714340.
2. Bishop, C.M. *Neural Networks for Pattern Recognition*; Clarendon Press: New York, NY, USA, 1995; ISBN 0198538642.
3. Hopfield, J.J.; Tank, D.W. Computing with neural circuits: A model. *Science* **1986**, *233*, 625–633. [CrossRef] [PubMed]
4. Strogatz, S.H. From Kuramoto to Crawford: Exploring the onset of synchronization in populations of coupled oscillators. *Phys. D Nonlinear Phenom.* **2000**, *143*, 1–20. [CrossRef]
5. Vodenicarevic, D.; Locatelli, N.; Abreu Araujo, F.; Grollier, J.; Querlioz, D. A Nanotechnology-Ready Computing Scheme based on a Weakly Coupled Oscillator Network. *Sci. Rep.* **2017**, *7*, 44772. [CrossRef] [PubMed]
6. Nakano, H.; Saito, T. Grouping Synchronization in a Pulse-Coupled Network of Chaotic Spiking Oscillators. *IEEE Trans. Neural Netw.* **2004**, *15*, 1018–1026. [CrossRef] [PubMed]

7. Velichko, A.; Belyaev, M.; Putrolaynen, V.; Pergament, A.; Perminov, V. Switching dynamics of single and coupled VO_2-based oscillators as elements of neural networks. *Int. J. Mod. Phys. B* **2017**, *31*, 1650261. [CrossRef]
8. Shukla, N.; Parihar, A.; Cotter, M.; Barth, M.; Li, X.; Chandramoorthy, N.; Paik, H.; Schlom, D.G.; Narayanan, V.; Raychowdhury, A.; Datta, S. Pairwise coupled hybrid vanadium dioxide-MOSFET (HVFET) oscillators for non-boolean associative computing. In Proceedings of the 2014 IEEE International Electron Devices Meeting, San Francisco, CA, USA, 15–17 December 2014; pp. 28.7.1–28.7.4.
9. Khitun, A.G.; Geremew, A.K.; Balandin, A.A. Transistor-Less Logic Circuits Implemented With 2-D Charge Density Wave Devices. *IEEE Electron. Device Lett.* **2018**, *39*, 1449–1452. [CrossRef]
10. Khitun, A.; Liu, G.; Balandin, A.A. Two-dimensional oscillatory neural network based on room-temperature charge-density-wave devices. *IEEE Trans. Nanotechnol.* **2017**, *16*, 860–867. [CrossRef]
11. Liu, G.; Debnath, B.; Pope, T.R.; Salguero, T.T.; Lake, R.K.; Balandin, A.A. A charge-density-wave oscillator based on an integrated tantalum disulfide-boron nitride-graphene device operating at room temperature. *Nat. Nanotechnol.* **2016**, *11*, 845–850. [CrossRef] [PubMed]
12. Ghosh, S. Generation of high-frequency power oscillation by astable mode arcing with SCR switched inductor. *IEEE J. Solid-State Circuits* **1984**, *19*, 269–271. [CrossRef]
13. Chen, C.; Mathews, R.; Mahoney, L.; Calawa, S.; Sage, J.; Molvar, K.; Parker, C.; Maki, P.; Sollner, T.C.L. Resonant-tunneling-diode relaxation oscillator. *Solid. State. Electron.* **2000**, *44*, 1853–1856. [CrossRef]
14. Sharma, A.A.; Bain, J.A.; Weldon, J.A. Phase Coupling and Control of Oxide-Based Oscillators for Neuromorphic Computing. *IEEE J. Explor. Solid-State Comput. Devices Circuits* **2015**, *1*, 58–66. [CrossRef]
15. Romera, M.; Talatchian, P.; Tsunegi, S.; Araujo, F.A.; Cros, V.; Bortolotti, P.; Yakushiji, K.; Fukushima, A.; Kubota, H.; Yuasa, S.; et al. Vowel recognition with four coupled spin-torque nano-oscillators. *arXiv*, 2018; arXiv:1711.02704.
16. Belyaev, M.A.; Boriskov, P.P.; Velichko, A.A.; Pergament, A.L.; Putrolainen, V.V.; Ryabokon', D.V.; Stefanovich, G.B.; Sysun, V.I.; Khanin, S.D. Switching Channel Development Dynamics in Planar Structures on the Basis of Vanadium Dioxide. *Phys. Solid State* **2018**, *60*, 447–456. [CrossRef]
17. Velichko, A.; Belyaev, M.; Putrolaynen, V.; Perminov, V.; Pergament, A. Thermal coupling and effect of subharmonic synchronization in a system of two VO_2 based oscillators. *Solid State Electron.* **2018**, *141*, 40–49. [CrossRef]
18. Sakai, J. High-efficiency voltage oscillation in VO_2 planer-type junctions with infinite negative differential resistance. *J. Appl. Phys.* **2008**, *103*, 103708. [CrossRef]
19. Hoppensteadt, F.C.; Izhikevich, E.M. Oscillatory Neurocomputers with Dynamic Connectivity. *Phys. Rev. Lett.* **1999**, *82*, 2983–2986. [CrossRef]
20. Hoppensteadt, F.C.; Izhikevich, E.M. Pattern recognition via synchronization in phase-locked loop neural networks. *IEEE Trans. Neural Netw.* **2000**, *11*, 734–738. [CrossRef] [PubMed]
21. Izhikevich, E.M. Weakly pulse-coupled oscillators, FM interactions, synchronization, and oscillatory associative memory. *IEEE Trans. Neural Netw.* **1999**, *10*, 508–526. [CrossRef] [PubMed]
22. Nikonov, D.E.; Csaba, G.; Porod, W.; Shibata, T.; Voils, D.; Hammerstrom, D.; Young, I.A.; Bourianoff, G.I. Coupled-Oscillator Associative Memory Array Operation for Pattern Recognition. *IEEE J. Explor. Solid-State Comput. Devices Circuits* **2015**, *1*, 85–93. [CrossRef]
23. Pikovsky, A.; Rosenblum, M.; Kurths, J. *(Jürgen) Synchronization: A Universal Concept in Nonlinear Sciences*; Cambridge University Press: Cambridge, UK, 2003; ISBN 9780521533522.
24. Theodoridis, S.; Koutroumbas, K. *Pattern Recognition*; Academic Press: Cambridge, MA, USA, 2009; ISBN 9781597492720.
25. Kumar, A.; Mohanty, P. Autoassociative Memory and Pattern Recognition in Micromechanical Oscillator Network. *Sci. Rep.* **2017**, *7*, 411. [CrossRef] [PubMed]
26. Shukla, N.; Parihar, A.; Freeman, E.; Paik, H.; Stone, G.; Narayanan, V.; Wen, H.; Cai, Z.; Gopalan, V.; Engel-Herbert, R.; et al. Synchronized charge oscillations in correlated electron systems. *Sci. Rep.* **2014**, *4*, 4964. [CrossRef]
27. Hoppensteadt, F.C.; Izhikevich, E.M. Synchronization of laser oscillators, associative memory, and optical neurocomputing. *Phys. Rev. E* **2000**, *62*, 4010–4013. [CrossRef]
28. Velichko, A.; Putrolaynen, V.; Belyaev, M. Effects of Higher Order and Long-Range Synchronizations for Classification and Computing in Oscillator-Based Spiking Neural Networks. *arXiv*, **2018**; arXiv:1804.03395.

29. Gill, P.E.; Murray, W.; Wright, M.H. *Practical Optimization*; Emerald Group Publishing: Bingley, UK, 1982; ISBN 0122839528.
30. Velichko, A.; Belyaev, M.; Putrolaynen, V.; Perminov, V.; Pergament, A. Modeling of thermal coupling in VO_2-based oscillatory neural networks. *Solid State Electron.* **2018**, *139*, 8–14. [CrossRef]